

Quasiballistic quantum transport through Ge/Si core/shell nanowires

D. Kotekar-Patil¹‡, B.-M. Nguyen²§, J. Yoo², S. A. Dayeh³,⁴
⁵, S. M. Frolov¹

¹ Department of Physics and Astronomy, University of Pittsburgh, Pittsburgh PA, 15260, USA

² Center for Integrated Nanotechnologies, Los Alamos National Laboratory, Los Alamos, NM 87545, USA

³ Department of Electrical and Computer Engineering, University of California, San Diego, La Jolla, CA 92037, USA

⁴ Graduate Program of Materials Science and Engineering, University of California, San Diego, La Jolla, CA 92037, USA

⁵ Department of NanoEngineering, University of California, San Diego, La Jolla, CA 92037, USA

E-mail: dpatil@tnu.edu.sg

Abstract.

We study signatures of ballistic quantum transport of holes through Ge/Si core/shell nanowires at low temperatures. We observe Fabry-Pérot interference patterns as well as conductance plateaus at integer multiples of $2e^2/h$ at zero magnetic field. Magnetic field evolution of these plateaus reveals relatively large effective Landé g-factors. Ballistic effects are observed in nanowires with silicon shell thicknesses of 1 - 3 nm, but not in bare germanium wires. These findings inform the future development of spin and topological quantum devices which rely on ballistic subband-resolved transport.

1. Introduction

A surge of interest in devices based on nanowires with strong spin-orbit interaction is due to their relevance for quantum computing [1, 2, 3, 4, 5, 6, 7] and for the realization of topological superconductivity and Majorana fermions [8, 9]. In this context, spin-orbit interaction in germanium/silicon nanowires was predicted and estimated experimentally to be strong [10, 11, 12, 13, 14, 15], superconducting contacts to these nanowires were demonstrated [16, 17], and large Landé g-factors were reported [18, 14]. Moreover, mobility upto $4200 \text{ cm}^2/\text{Vs}$ was reported in these nanowires [19]. These effects, provided

‡ Present address: Division of Physics and Applied Physics, Nanyang Technological University, Singapore

§ Present address: HRL Laboratories, 3011 Malibu Canyon Road, Malibu, California 90265, USA

they are observed in the ballistic transport regime [20, 21, 22], are essential for Majorana experiments.

In this paper, we report transconductance resonances consistent with one-dimensional (1D) subbands occupied one-by-one as the top gate voltage is made more negative. At low temperatures (<1 K) transport is strongly dominated by Fabry-Pérot interference patterns. The magnetic field evolution of conductance resonances reveals large g-factors. These effects are observed for a range of silicon shell thicknesses without any obvious dependence on shell thickness of silicon shell thickness, however devices without any shell did not show ballistic transport signatures and exhibited substantial charge instabilities. We estimate the subband spacing to be ~ 20 meV, the low temperature mobility of up to 1000 cm²/Vs and the mean free path of 70 nm. The mean free path is larger than the core diameter consistent with the quasiballistic regime.

2. Fabrication

Ge/Si core/shell nanowires (NWs) are grown using the low pressure, cold-walled chemical vapor deposition. NWs are grown with various core diameters ($15 - 55$ nm) and shell thicknesses ($0 - 4$ nm) [23]. Fig. 1a shows a high resolution transmission electron micrograph of a Ge/Si core/shell NW demonstrating a high degree of control over the silicon shell thickness [24, 25, 26]. To fabricate devices, the NWs are sonicated in isopropanol and then dropped onto Si₃N₄ substrates with alignment markers. In order to achieve the low ohmic contact resistance, a dip in hydrofluoric acid is performed to etch the native oxide on the silicon shell. Electron beam evaporation and electron beam lithography are used to define two 150 nm thick nickel contacts. This step is followed by a 30 second rapid thermal annealing at 300°C . During annealing, Ni diffuses into the NW from both ends forming highly doped NiGe_{*x*}/NiSi_{*y*} ohmic contacts [27, 28, 29]. Segments of the NW between the sections of NiGe_{*x*}/NiSi_{*y*} define the Ge/Si channel length ($L = 250 - 450$ nm). As a last step, a top gate stack consisting of a 10 nm thick hafnium oxide gate dielectric is deposited using atomic layer deposition and then a 30 nm/ 100 nm thick Ti/Au top gate electrode is evaporated. Gate contact overlaps with the NiGe_{*x*}/NiSi_{*y*} region fully covering the unannealed Ge/Si channel.

3. Signatures of conductance quantization

Electrical characterization is performed in a dilution refrigerator equipped with a 9 T magnet, using a standard lock-in technique at 27 Hz with an excitation voltage of 50 μV . Noise attenuation is done in 2 stages: at room temperature using π -filters, and at low temperatures using two-stage low-pass RC filters. Room temperature characterization of the same devices is reported by Nguyen et al.[23]. The room temperature saturation resistance, which is the two-terminal resistance measured at highly negative top gate voltages (V_g), is in the range of 10 k Ω . The room temperature field effect mobility is

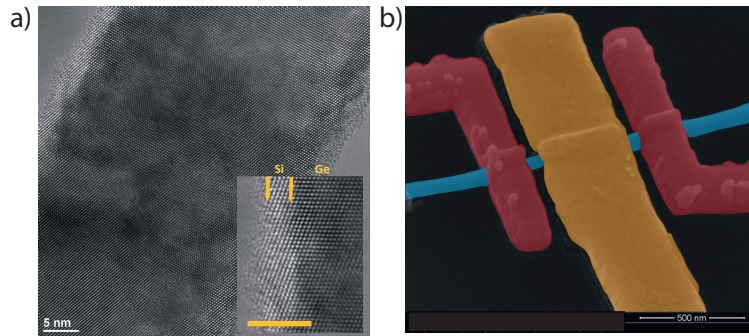


Figure 1. (a) High resolution transmission electron micrograph of a Ge/Si nanowire. Inset shows a well-defined interface between the Si shell and the Ge core. (b) False color scanning electron micrograph of a device where blue region corresponds to the NW, red regions correspond to the source and drain contacts, yellow region corresponds to the top Ti/Au gate.

150 - 250 cm^2/Vs for NWs with silicon shells independent of shell thickness, and 50 cm^2/Vs for bare Ge NWs. Measurements in this work show that at low temperatures the saturation resistance is comparable to the room temperature resistance (1 - 20 $\text{k}\Omega$). The low temperature field-effect mobility is in the range of 200 - 500 cm^2/Vs with the highest mobility of 1000 cm^2/Vs extracted from the pinch-off traces using gate-to-nanowire capacitance calculated by a self-consistent Poisson solver (see supplementary information).

As gate voltage is swept from positive to negative, conductance increases in steps of $2e^2/h$ (Fig. 2a). We associate this with one-dimensional spin-degenerate subband-resolved transport. Additionally, we observe a conductance plateau below the first $2e^2/h$ plateau. Such features are frequently reported in quantum point contacts [30, 31, 32, 33] and are not the focus of this work. We further investigate this device in the non-linear regime where conductance through the NW is studied as a function of bias voltage (V) and gate voltage. Fig. 2b shows the waterfall plot in which we observe accumulations of conductance traces near $2e^2/h$ and $4e^2/h$. However, plateaus at $0.5 \times 2e^2/h$ that are expected in quantum point contacts at high bias, when the bias exceeds the subband spacing, could not be resolved due to strong current fluctuations at high bias.

Fig. 2c shows the transconductance (dG/dV_g) of the data in the panel 2b. High transconductance resonances move linearly as a function of V_g and V . The difference in bias between points where positive and negative slope transconductance resonances meet (forming diamond-shaped regions) indicate the energy separation between the 1D subbands. From Fig. 2c, we observe that the first (E_{2-1}) and second (E_{3-2}) transconductance diamonds have approximately the same size of ≈ 22 meV. This energy separation is consistent with transverse quantization in the nanowire for heavy holes with an effective mass of $m_{hh} = 0.28m_e$, where m_e is the free electron mass. Additionally, the slopes of the transconductance resonances are used to extract the gate lever arm parameter $\alpha = dV/dV_g = 29.5$ meV/V.

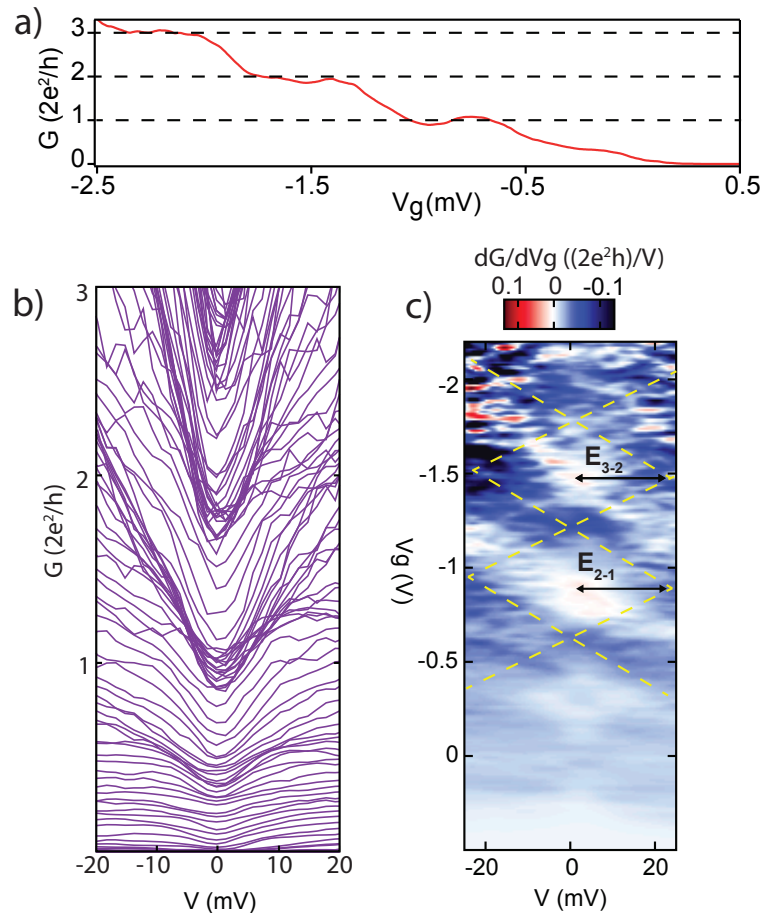


Figure 2. (a) Conductance G as a function of gate voltage V_g , at $V = 0$ V. (b) Waterfall plot of conductance: each trace is taken at a fixed $V_g = 0.5 - (-2.5)$ V. There is no offset between the traces. (c) Transconductance dG/dV_g of the data in panel (b) with high transconductance resonances marked by dashed lines. Energy splittings deduced from transconductance resonances are indicated by solid arrows. All data obtained at zero applied magnetic field, $T = 5.5$ K; a series resistance of 21 k Ω is subtracted.

4. Magnetotransport

Fig. 3 shows the evolution of conductance steps as a function of magnetic field. We note that we only observe Zeeman splitting for the second and third conductance steps while the first step only exhibits a Zeeman shift rather than a splitting. In addition, there are other resonances in fig. 3 which move linearly with magnetic field. We associate these resonances to quantum interference effects [34], similar g -factors can be extracted for these resonances. Zeeman splitting is given by $\Delta E_z = g \mu_B B$, where μ_B is the Bohr's magneton. We use the lever arm parameter calculated from the transconductance diamond in Fig. 2c to convert the V_g axis into the energy scale. This gives a g -factor for each transition which we denote by $g_1=2$ for the first transition, $g_2=10.7 \pm 2.3$ for transition between the first and the second conductance steps and $g_3=4.7 \pm 1.3$ for transition between the second and the third conductance step.

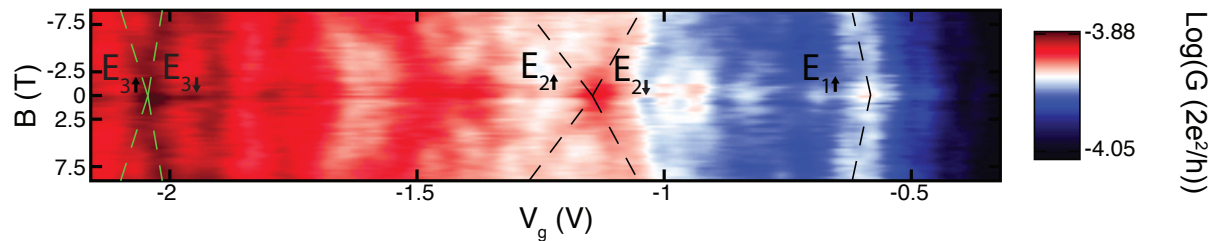


Figure 3. Differential conductance as a function of magnetic field and V_g at $V = 0V$ for field oriented at an angle of 45° to the nanowire. Black dashed lines mark the spin splitting of the first ($E_{1\uparrow}$) and second conductance step ($E_{2\downarrow}$ and $E_{2\uparrow}$) and green dashed lines mark spin splitting of the third conductance step ($E_{3\downarrow}$ and $E_{3\uparrow}$).

Due to the large effective hole masses, the orbital effects of magnetic field are ignored when extracting g-factors, however they may contribute to the shifts of resonances in magnetic field, especially for the resonances with the smaller apparent g-factors. Large g-factors were also recently observed in Ge/Si nanowire quantum dots [18, 14].

5. Fabry-Pérot interference

While all devices are fabricated following the same process, of 45 measured devices, only two show signatures of conductance quantization (shown in fig.2 and S1). In a typical device, subband-resolved transport and conductance plateaux are scrambled due to backscattering and are replaced with Fabry-Perot interference within the channel (Fig. 4a). This device is based on a NW with diameter $d = 35$ nm, length $L = 350$ nm and shell thickness $t_{si} = 1$ nm at $T = 400$ mK. Mobility extracted from $G(V_g)$ trace at $T = 4$ K is ≈ 450 cm^2/Vs . While this trace does not show conductance plateaux, it is a representative trace for many core/shell devices studied at temperatures below 1 K. With the application of negative gate voltage, conductance reaches $4e^2/h$ indicating transport through at least two subbands. In the whole V_g range shown in Fig. 4a, conductance trace exhibits quasi-periodic oscillations. The smallest period measured in V_g is approximately $\Delta V_g \approx 9$ mV. Fig. 4b shows the evolution of these quasi-periodic conductance oscillations as a function of V_g and V : the zero-bias features evolve into checkerboard patterns at finite bias. We attribute this to Fabry-Pérot interference [35, 22]. The energy spacing of Fabry-Pérot resonances $\Delta E = 1 - 2$ meV (fig.4c) is linked to the cavity L_c length by: $\Delta E = \frac{\hbar^2 \pi^2}{2m^* L_c^2} \approx 75\text{-}110$ nm. This implies that the segment of NW over which Fabry-Pérot interference takes place is approximately one-third of the NW channel.

To conclude, signatures compatible with conductance quantization are measured in Ge/Si NW devices. Magnetic field dependence reveals that the hole g-factor in our NWs is large and exhibits strong anisotropy. Moreover, the presence of a silicon shell on the NW results in quasiballistic transport which is absent in bare Ge NW (see supplementary).

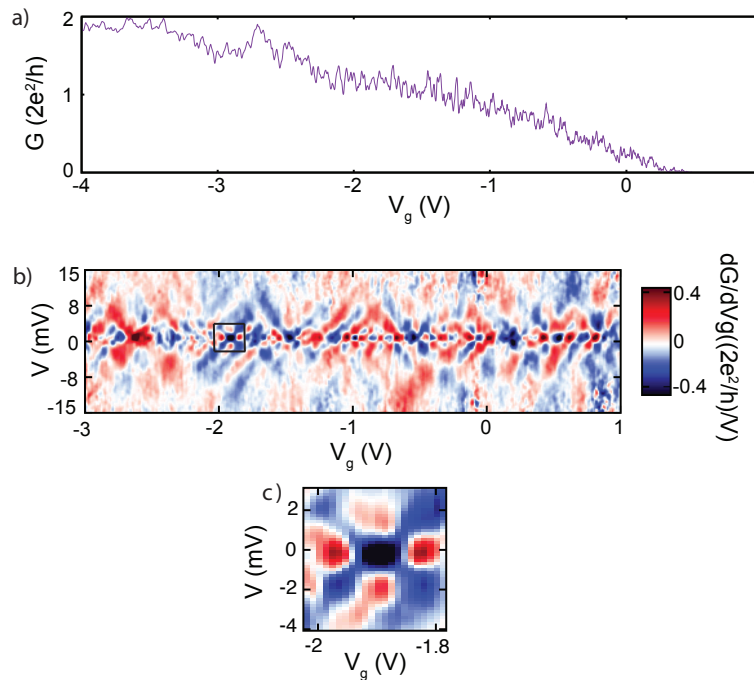


Figure 4. (a) Differential conductance at $V = 0$ V and (b) transconductance map for a device with silicon shell thickness of 1 nm. $T = 400$ mK, $B = 0$ T (c) zoom-in of the checkerboard pattern marked by black box in panel (b).

6. Acknowledgement

The Ge/Si nanowire growth was performed at the Center for Integrated Nanotechnologies (CINT), U.S. Department of Energy, Office of Basic Energy Sciences User Facility at Los Alamos National Laboratory (Contract DE-AC52-06NA25396) and Sandia National Laboratories (Contract DE-AC04-94AL85000). We thank Z. Su and A. Zarassi for technical help and useful discussions. S.A.D. acknowledges NSF support under DMR-1503595 and ECCS-1351980. S.M.F. acknowledges NSF DMR-125296, ONR N00014-16-1-2270 and Nanoscience Foundation, Grenoble.

7. References

- [1] Nadj-Perge S, Frolov S M, Bakkers E P A M and Kouwenhoven L P 2010 *Nature* **468** 1084–1087 ISSN 0028-0836 URL <http://dx.doi.org/10.1038/nature09682>
- [2] Pribiag V S, Nadj-Perge S, Frolov S M, van den Berg J W G, van Weperen I, Plissard R, Bakkers M P A and Kouwenhoven L 2013 *Nat Nano* **8** 170–174 ISSN 1748-3387 URL <http://dx.doi.org/10.1038/nnano.2013.5>
- [3] Veldhorst M, Yang C H, Hwang J C C, Huang W, Dehollain J P, Muhonen J T, Simmons S, Laucht A, Hudson F E, Itoh K M, Morello A and Dzurak A S 2015 *Nature* **526** 410–414 ISSN 0028-0836 URL <http://dx.doi.org/10.1038/nature15263>
- [4] Patil D K, Corna A, Maurand R, Crippa A, Orlov A, Barraud S, Jehl X, De Franceschi S and Sanquer M 2016 *arXiv preprint arXiv:1606.05855*
- [5] Maurand R, Jehl X, Patil D K, Corna A, Bohuslavskiy H, Laviéville R, Hutin L, Barraud S, Vinet M, Sanquer M and De Franceschi S 2016 *arXiv preprint arXiv:1605.07599*

- [6] Bohuslavskiy H, Kotekar-Patil D, Maurand R, Corna A, Barraud S, Bourdet L, Hutin L, Niquet Y M, Jehl X, De Franceschi S, Vinet M and Sanquer M 2016 *Applied Physics Letters* **109** 193101 URL <http://scitation.aip.org/content/aip/journal/apl/109/19/10.1063/1.4966946>
- [7] Higginbotham A P, Larsen T W, Yao J, Yan H, Lieber C M, Marcus C M and Kuemmeth F 2014 *Nano Letters* **14** 3582–3586 pMID: 24797219 (*Preprint* <http://dx.doi.org/10.1021/nl501242b>) URL <http://dx.doi.org/10.1021/nl501242b>
- [8] Mourik V, Zuo K, Frolov S M, Plissard S R, Bakkers E P A M and Kouwenhoven L P 2012 *Science* **336** 1003–1007 ISSN 0036-8075 (*Preprint* <http://science.sciencemag.org/content/336/6084/1003.full.pdf>) URL <http://science.sciencemag.org/content/336/6084/1003>
- [9] Albrecht S M, Higginbotham A P, Madsen M, Kuemmeth F, Jespersen T S, Nygard J, Krogstrup P and Marcus C M 2016 *Nature* **531** 206–209 ISSN 0028-0836 URL <http://dx.doi.org/10.1038/nature17162>
- [10] Kloeffer C, Trif M and Loss D 2011 *Phys. Rev. B* **84**(19) 195314 URL <http://link.aps.org/doi/10.1103/PhysRevB.84.195314>
- [11] Hu Y, Churchill H O H, Reilly D J, Xiang J, Lieber C M and Marcus C M 2007 *Nat Nano* **2** 622–625 ISSN 1748-3387 URL <http://dx.doi.org/10.1038/nnano.2007.302>
- [12] Hao X J, Tu T, Cao G, Zhou C, Li H O, Guo G C, Fung W Y, Ji Z, Guo G P and Lu W 2010 *Nano Letters* **10** 2956–2960 pMID: 20698609 (*Preprint* <http://dx.doi.org/10.1021/nl101181e>) URL <http://dx.doi.org/10.1021/nl101181e>
- [13] Brauns M, Ridderbos J, Li A, Bakkers E P A M, van der Wiel W G and Zwanenburg F A 2016 *Phys. Rev. B* **94**(4) 041411 URL <http://link.aps.org/doi/10.1103/PhysRevB.94.041411>
- [14] Zarassi A, Su Z, Danon J, Schwenderling J, Hocevar M, Nguyen B M, Yoo J, Dayeh S A and Frolov S M 2016 *ArXiv e-prints* (*Preprint* 1610.04596)
- [15] Maier F, Klinovaja J and Loss D 2014 *Phys. Rev. B* **90**(19) 195421 URL <http://link.aps.org/doi/10.1103/PhysRevB.90.195421>
- [16] Xiang J, Vidan A, Tinkham M, M W and Lieber C M 2006 *Nat Nano* **1** 208–213
- [17] Su Z, Zarassi A, Nguyen B M, Yoo J, Dayeh S A and Frolov S M 2016 *ArXiv e-prints* (*Preprint* 1610.03010)
- [18] Brauns M, Ridderbos J, Li A, Bakkers E P A M and Zwanenburg F A 2016 *Phys. Rev. B* **93**(12) 121408 URL <http://link.aps.org/doi/10.1103/PhysRevB.93.121408>
- [19] Conesa-Boj S, Li A, Koelling S, Brauns M, Ridderbos J, Nguyen T T, Verheijen M A, Koenraad P M, Zwanenburg F A and Bakkers E P A M 2017 *Nano Letters* **17** 2259–2264 pMID: 28231017 (*Preprint* <http://dx.doi.org/10.1021/acs.nanolett.6b04891>) URL <http://dx.doi.org/10.1021/acs.nanolett.6b04891>
- [20] van Weperen I, Plissard S R, Bakkers E P A M, Frolov S M and Kouwenhoven L P 2013 *Nano Letters* **13** 387–391 pMID: 23259576 (*Preprint* <http://dx.doi.org/10.1021/nl3035256>) URL <http://dx.doi.org/10.1021/nl3035256>
- [21] Lu W, Xiang J, Timko B P, Wu Y and Lieber C M 2005 *Proceedings of the National Academy of Sciences of the United States of America* **102** 10046–10051 (*Preprint* <http://www.pnas.org/content/102/29/10046.full.pdf>) URL <http://www.pnas.org/content/102/29/10046.abstract>
- [22] Kretinin A V, Popovitz-Biro R, Mahalu D and Shtrikman H 2010 *Nano Letters* **10** 3439–3445 pMID: 20695446 (*Preprint* <http://dx.doi.org/10.1021/nl101522j>) URL <http://dx.doi.org/10.1021/nl101522j>
- [23] Nguyen B M, Taur Y, Picraux S T and Dayeh S A 2014 *Nano Letters* **14** 585–591 pMID: 24382113 (*Preprint* <http://dx.doi.org/10.1021/nl4037559>) URL <http://dx.doi.org/10.1021/nl4037559>
- [24] Dayeh S A, Gin A V and Picraux S T 2011 *Applied Physics Letters* **98** 163112 URL <http://scitation.aip.org/content/aip/journal/apl/98/16/10.1063/1.3574537>
- [25] Dayeh S A, Mack N H, Huang J Y and Picraux S T 2011 *Applied Physics Letters* **99** 023102 URL <http://scitation.aip.org/content/aip/journal/apl/99/2/10.1063/1.3567932>

- [26] Dayeh S A, Tang W, Boioli F, Kavanagh K L, Zheng H, Wang J, Mack N H, Swadener G, Huang J Y, Miglio L, Tu K N and Picraux S T 2013 *Nano Letters* **13** 1869–1876 pMID: 23030346 (*Preprint* <http://dx.doi.org/10.1021/nl3022434>) URL <http://dx.doi.org/10.1021/nl3022434>
- [27] Wu Y, Xiang J, Yang C, Lu W and Lieber C M 2004 *Nature* **430** 61–65 ISSN 0028-0836 URL <http://dx.doi.org/10.1038/nature02674>
- [28] Tang W, Nguyen B M, Chen R and Dayeh S A 2014 *Semiconductor Science and Technology* **29** 054004 URL <http://stacks.iop.org/0268-1242/29/i=5/a=054004>
- [29] Dayeh S, Tang W, Nguyen B M, Dai X, Liu Y, Hwang Y, Liu X H and Chen R 2013 *ECS Transactions* **58** 115–125 (*Preprint* <http://ecst.ecsdl.org/content/58/7/115.full.pdf+html>) URL <http://ecst.ecsdl.org/content/58/7/115.abstract>
- [30] Thomas K J, Nicholls J T, Simmons M Y, Pepper M, Mace D R and Ritchie D A 1996 *Phys. Rev. Lett.* **77**(1) 135–138 URL <http://link.aps.org/doi/10.1103/PhysRevLett.77.135>
- [31] Cronenwett S M, Lynch H J, Goldhaber-Gordon D, Kouwenhoven L P, Marcus C M, Hirose K, Wingreen N S and Umansky V 2002 *Phys. Rev. Lett.* **88**(22) 226805 URL <http://link.aps.org/doi/10.1103/PhysRevLett.88.226805>
- [32] Reilly D J, Buehler T M, O'Brien J L, Hamilton A R, Dzurak A S, Clark R G, Kane B E, Pfeiffer L N and West K W 2002 *Phys. Rev. Lett.* **89**(24) 246801 URL <http://link.aps.org/doi/10.1103/PhysRevLett.89.246801>
- [33] Komijani Y, Csontos M, Shorubalko I, Ihn T, Ensslin K, Meir Y, Reuter D and Wieck A D 2010 *EPL (Europhysics Letters)* **91** 67010 URL <http://stacks.iop.org/0295-5075/91/i=6/a=67010>
- [34] Lundeberg M B and Folk J A 2009 *Nat Phys* **5** 894–897 ISSN 1745-2473 URL <http://dx.doi.org/10.1038/nphys1421>
- [35] Biercuk M J, Mason N, Martin J, Yacoby A and Marcus C M 2005 *Phys. Rev. Lett.* **94**(2) 026801 URL <http://link.aps.org/doi/10.1103/PhysRevLett.94.026801>